Visualizing Heterogeneity of Monodisperse CdSe Nanocrystals by Their Assembly into Three-Dimensional Supercrystals

Elena V. Shevchenko,[1*] Paul Podsiadlo,[1,2] Xiaohua Wu,[1,3] Byeongdu Lee,[4] Tijana Rajh,[1]

Rachel Morin,[5] Matthew Pelton[1,5*]

[1]*Center for Nanoscale Materials, Argonne National Laboratory, 9700 South Cass Avenue, Argonne, Illinois 60439, United States.*

[2]*ExxonMobil Research and Engineering Company, Fuels, Process & Optimization Technology Process Engineering Division, 22777 Springwoods Village Parkway Spring, TX 77389, United States.*

[3]*Mindray, Mindray Building, Hitech Industrial park, Nanshan District, Shenzhen, China*

[4]*Advanced Photon Source, Argonne National Laboratory, 9700 South Cass Avenue, Argonne, Illinois 60439, United States.*

[5]*Department of Physics, UMBC (University of Maryland, Baltimore County), 1000 Hilltop Circle, Baltimore, MD 20912, United States.*

[*] Corresponding authors: eshevchenko@anl.gov; mpelton@umbc.edu

ABSTRACT

The small energy difference between the (cubic) zinc blende and (hexagonal) wurzite phases of CdSe makes it challenging to synthesize ensembles of CdSe nanocrystals that all have the same, single crystalline phase. Although several different synthetic protocols have been proposed to provide a better control over crystalline phase, the contribution of polymorphism to self-assembly of CdSe nanocrystals has so far been ignored. Here, we investigate the self-assembly of monodisperse CdSe nanocrystals synthesized at lower temperature (~310 ^{o}C). We show that their assembly into three-dimensional superlattices results in the formation of separate regions within the superlattices that display photoluminescence at two distinctly different wavelengths. Specifically, the central portions of the supercrystals displayed photoluminescence and absorption in the orange region of the spectrum, around 585 nm, compared to the 575-nm photoluminescence maximum for the nanocrystals dispersed in toluene. Distinct domains on the surfaces and edges of the supercrystals, by contrast, displayed photoluminescence and absorption in the green region of the spectrum, around 570 nm. We attribute the different-colored domains to polytypism in the nanocrystal ensembles: the "orange" regions are primarily formed from wurtzite nanocrystals, and the "green" regions are formed from CdSe nanocrystals with zinc-blende phase. We hypothesize that lower surface coverage of zinc-blende CdSe nanocrystals, compared to that of the wurtzite nanocrystals, results in weaker protection of these nanocrystals against oxidation, and that this oxidation is responsible for the observed blue shift in photoluminescence and absorption. By contrast, we show that superlattices formed out of single-phase CdSe nanocrystals synthesized at higher temperature (~380 ^{o}C) do not contain the two differently-colored domains. Our observation provides a straightforward method to visualize polytypism in nanocrystal ensembles and understand its impact on nanocrystal self-assembly.

Keywords: self-assembly, CdSe, nanocrystals, superlattices, photoluminescence, electronic coupling, polytypism, polymorphism

TOC GRAPHIC

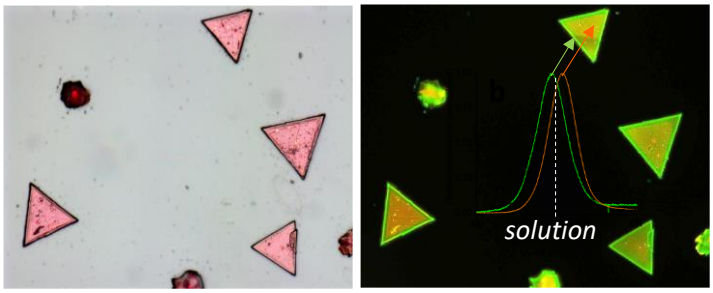

The synthesis of monodisperse spherical CdSe nanocrystals (NCs)[1] led shortly afterwards to their use as building blocks for more complex, hierarchical structures, such as ordered three-dimensional (3D) assemblies. Since the first report of 3D assembly in 1995,[2] CdSe NCs with different shapes such as nanorods, tetrapods, or even atomically flat nanoplates have been synthesized in solution and organized from the solution into 3D assemblies,[3-8] driven by interactions among neighboring particles.[9]

Periodic NC structures can be obtained by evaporation of the solvent[10-14] or by the destabilization of the colloidal solution by non-solvent.[15-18] Solvent evaporation typically enables the fabrication of continuous long-range periodic films, whereas solution destabilization[15, 19] results in the growth of 3D supercrystals (SCs) with symmetries similar to those of atomic inorganic crystals.[17, 20] Monodisperse NCs can form face-centered cubic (fcc),[17] body-centered cubic (bcc),[17] simple hexagonal,[21] face-centered tetragonal (fct), and other lattices. Multicomponent mixtures enable the creation of an extended library of periodic structures isostructural with atomic lattices.[11-12, 22-23] In multicomponent mixtures, NCs can have the same or different surface chemistries, sizes, and composition. However, the effects of polytypism on self-assembly has so far remained unexplored. An open question is how particles with the same size, composition, and capping molecules but with different phases (*i.e.*, different crystal structures) will assemble.

Polytypism is known to be common in II-VI semiconducting NCs, which can present both in cubic zinc blende (ZB) and hexagonal wurzite (W) crystalline phases.[24] For CdSe, the energy difference between ZB and W is only 1.4 meV/atom,[25] which makes synthesis of the pure crystalline phase NCs challenging.[26-27] The ratio of the ZB and W phase is very sensitive to the experimental conditions, such as the choice of surface ligands.[20, 26, 28-31] Indeed, transitions between

the ZB and W phases can be induced by introducing different ligands[26, 29] or by changing the NC surface.[32] The phase of CdSe NCs can depend even on the length of the ligands.{Huang, 2010 #686} Moreover, individual NCs can have stacking faults which locally induce a phase change, and hence, both phases can be present in the same NCs.[28,33] Conversely, NCs of the same size and composition but with different phases can have different ligand coverages of their surfaces; this, in turn, can influence the solvation of their ligand shells[34] and thus the interactions among NCs.[35-37] Since ligand-ligand interactions are one of the key factors determining the NC self-assembly process,[7, 38-40] polytypism has the potential to significantly affect CdSe NC self-assembly.

Here, we report an unusual optical effect in individual 3D SCs assembled by the destabilization of a solution of monodisperse CdSe NCs. The majority of each supercrystal emits light that is red-shifted as compared to the corresponding NC solution, while some outer regions of the supercrystals emit blue-shifted light. (For the nanocrystal sizes we used, these correspond to red-emitting and green-emitting regions.) We attribute the bimodal light emission to the polytypism of CdSe NCs synthesized in a mixture of TOPO, TOP, and HDA. We suggest that the surface of CdSe NC with ZB phase s in the SCs is less protected as compared to the surfaces of W NCs. As a result, such ZB NCs tend to oxidize more easily, moving their emission to shorter wavelengths. The difference in surface-ligand coverage also drives the separation of these ZB NCs from the W NCs during the self-assembly process, leading to distinct spatial regions with different crystal structures and different emission wavelengths.

RESULTS AND DISCUSSION

Figures 1a and S1 show TEM images of monodisperse 4.4- and 4.6-nm CdSe NCs stabilized with TOPO, TOP and HDA,[1935] and Figure 1b shows the corresponding narrow absorption spectra.

Gentle destabilization of colloidal solutions of these NCs resulted in the formation of supercrystals of various shapes, with lateral dimensions up to 80 μm (Figure 1c,e).[16-17] SEM images of SCs are shown in Figure S3. Such SCs were previously reported to have a face-centered cubic lattice structure.[17]

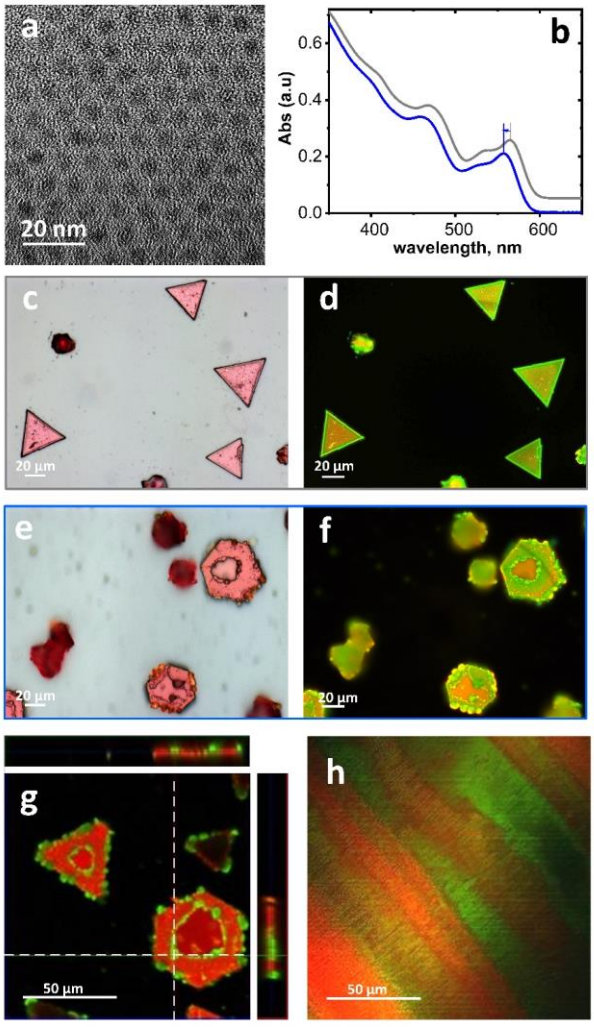

Figure 1. *(a) Transmission-electron micrograph of 4.6-nm CdSe nanocrystals. (b) Absorption spectra of dilute solutions of 4.4-nm (grey curve) and 4.6-nm (blue curve) CdSe nanocrystals in toluene. (c-f) Representative reflected-light optical micrographs (c,e) and corresponding fluorescence micrographs (d,f) of several three-dimensional supercrystals formed from 4.4-nm (c,d) and 4.6-nm (e,f) CdSe nanocrystals by controlled destabilization of the solution. (g) Laser-scanning confocal micrograph of supercrystals; side images are cross-sections along the indicated lines. (h) Laser-scanning confocal micrograph of a dried film of the nanocrystals.*

Fluorescence images of individual SCs revealed a surprising coexistence of green-emitting and orange-emitting regions (Figure 1d,f). The green regions are distinctly localized along the edges and within the interior of the assemblies (Figure S4). Comparison of the reflected-light and fluorescence images clearly shows the integrity of the different regions. 3D composite images obtained from laser scanning confocal microscopy (Figure 1g) show that the different regions penetrate through the interior of the SCs and all the way to the substrate. The green regions appear less ordered in the fluorescence and confocal images, having irregular shapes and boundaries compared to the faceted appearance of the orange regions. In addition, randomly packed films of the same 4.4-nm NCs also exhibited red- and green-emitting regions (Figure 1h). We note that the NCs were washed before deposition of the disordered films so that the number of ligands in the films is similar to the number of ligands in the SCs, as confirmed by TGA (Figure S5).

Formatted: Font color: Red

To obtain more information about the optical properties of the “green” and “orange” regions, we made spatially resolved measurements of the PL and absorption spectra of the SCs. Compared to solutions of the same NCs, the “orange” regions of the SC exhibit both absorption and PL at lower energies, and the “green” regions exhibit both absorption and PL at higher energies (Figure 2a,b).

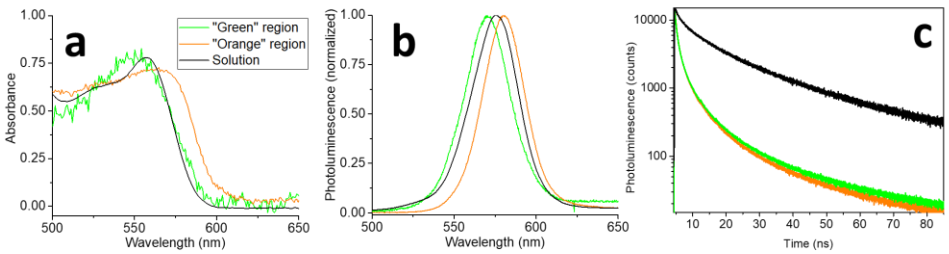

Figure 2: *Characteristic spatially resolved (a) absorbance spectra, (b) photoluminescence spectra, and (c) time-resolved photoluminescence decay curves for blue-shifted ("green") and red-shifted ("orange") regions within individual supercrystals formed from 4.4-nm CdSe nanocrystals. The microscopic measurements have a spatial resolution of approximately 200 nm. Also shown for comparison are results for nanocrystals dispersed in toluene solution.*

The red shift of the PL in the orange regions could potentially be attributed to energy transfer among the NCs in the SC[2, 41] or to luminescence from near-band-edge defect states.[42] However, these phenomena would not explain the red shift of the absorption in the same regions and are inconsistent with the symmetric PL spectra observed from all spots. Instead, we attribute the red shift to the local field effect; *i.e.*, to the higher dielectric constant of the NC environment in the SC as compared to solution.[43] This dielectric effect is consistent with the time-resolved PL dynamics, which show faster recombination rate for NCs in the SCs as compared to in solution (Figure 2c).[44]

On the other hand, the PL dynamics in the orange and green regions are nearly identical to one another. This indicates that the NCs in these two regions have nearly identical dielectric surroundings, so that differences in the dielectric environment are not responsible for differences in the PL and absorption wavelengths between the orange and green regions. The PL dynamics also provide further evidence that energy transfer, charge transfer, or trapping are not responsible for the different PL wavelengths in the different regions. Rather, we conclude that the NCs in the green regions have a higher effective bandgap (*i.e.*, higher confinement energy) than the NCs in

the orange regions. The clearest evidence for the altered effective bandgap is the blue shift of both the PL and absorption in the green regions.

Since the green regions tend to be located at the surfaces of the SCs, it could be hypothesized that the different colors are due to segregation of smaller NCs from larger NCs in solution, driven by depletion interactions.[45] Indeed, previous studies of CdSe NC SCs assembled from polydisperse colloidal solutions showed size selection of NCs during SC assembly.[46] However, analysis of the TEM images (Figures 1a, S1, S2) reveals no evidence of polydispersity in the NC samples that we used. Moreover, when we deliberately mixed solutions of different-sized NCs and formed SCs from these solutions, we observed only single-color SCs (Figure S6). That is, mixtures of NCs that are "orange" and "green" because of their different diameters form separate orange and green SCs, and do not form the two-color SCs that form from monodisperse NC solutions. We also note that there are only two distinct emission wavelengths for the two-color superlattices: different points within the "orange" regions all emitted at the same wavelength, and different points within the "green" regions all emitted at the same wavelength (Figure S7). This is different from the continuous variation in emission wavelength that one would expect to arise from size segregation of a polydisperse sample.

Formatted: Font color: Red

A second potential explanation for the different emission colors is a difference in the packing of NCs in the different regions of the SCs, which would lead to different electronic coupling among the NCs. However, spatially resolved SAXS measurements on individual SCs did not reveal significant changes in the packing of NCs between the orange and green regions (Figure 3).

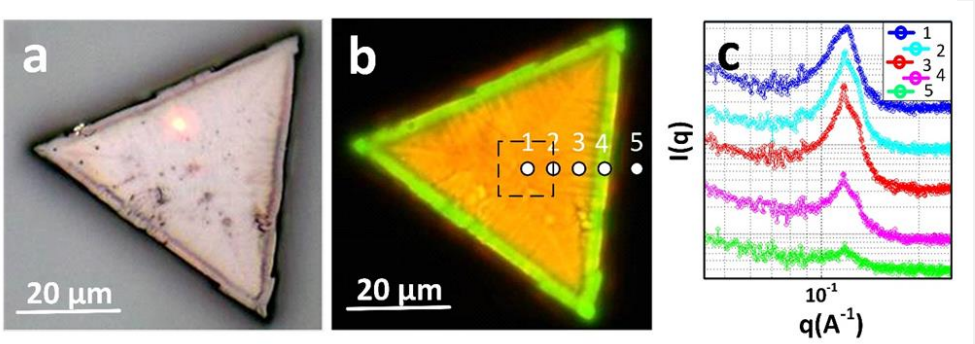

Figure 3. *(a,b) Reflected-light optical micrograph (a) and corresponding fluorescence image (b) of a supercrystal assembled from 4.6-nm CdSe nanocrystals. (c) Small-angle X-ray scattering spectra measured from five selected spots on the nanocrystal, as indicated in (b). The square represents the approximate size of the X-ray spot.*

Another possible explanation for the different emission colors is differences in strain within the orange and green regions. Indeed, it was previously reported that both absorption and PL spectra can be blue shifted by compressive strain of NCs,[41] and previous Raman microprobe studies have revealed large strains of ~2.5% for CdSe NCs in films.[47] Crack formation was proposed as a strain-relief mechanism for the films;[47] however, we observe two-color PL even from SCs with cracks (Figure 4a,b). Moreover, spatially resolved Raman spectroscopy shows no shift in the Raman peak position across the orange and green domains (Figures 4c,d), indicating the absence of strain within the CdSe NCs. Therefore, cracks are likely formed as a result of the evaporation of the solvent retained in the ligands' shells of the self-assembled NCs upon their drying.[30-39]

Field Code Changed

Field Code Changed

On the other hand, the fluorescence image of the SC after the spatially-resolved Raman measurement provides a clue about the origin of the green PL: a green line appears where the excitation laser was scanned across the sample (Figure 4b). This line is formed as a result of photooxidation of NCs in the SC.[48] Oxidation reduces the effective diameter of the NCs by

replacing a surface semiconductor layer with oxides,[49] thereby increasing the confinement energy and increasing the effective bandgap. This observation suggests that the NCs within the green regions of the SCs have oxidized compared to the NCs within the orange regions of the same SCs.

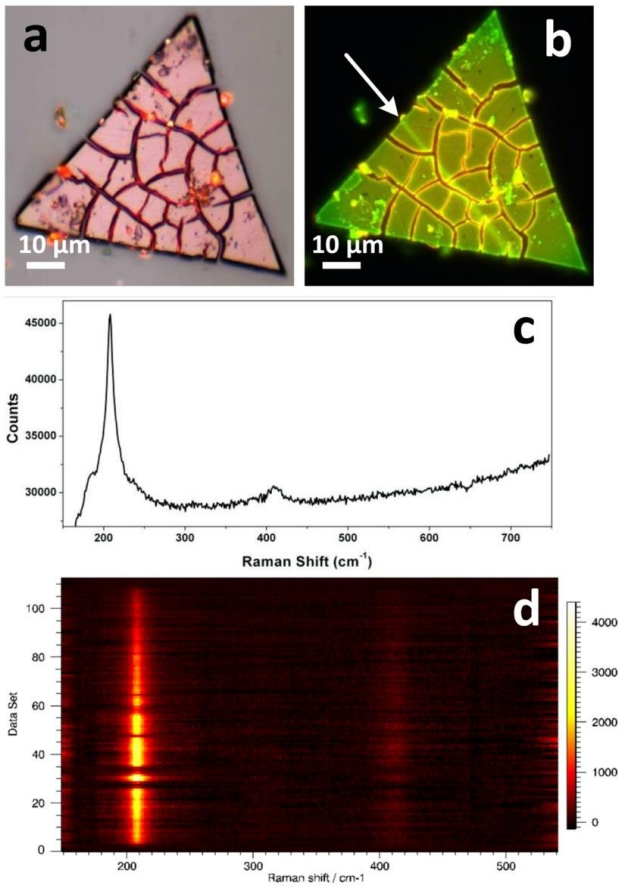

Figure 4. *(a-b) Reflected-light optical micrograph (a) and corresponding fluorescence image (b) of a supercrystal formed from 4.4-nm CdSe nanocrystals. (c) Representative Raman spectrum from the supercrystal, showing the CdSe LO (208 cm^{-1}), 2LO (420 cm^{-1}), and surface (188 cm^{-1}) phonon peaks. (d) Two-dimensional Raman-scattering intensity map taken along the line indicated by the white arrow in (b). Interruptions in the Raman map correspond to cracks in the SC. The fluorescence image in (b) was taken after the Raman map was acquired, and green emission can be seen along the path of the line.*

To verify this explanation, we treated our SCs with 0.01 M solution of pyridine in toluene for 1 h. Exposure of CdSe SCs to pyridine solution is known to reduce the protection of the surfaces of CdSe NCs and thus make the surfaces more easily oxidized.[50] Indeed, the two-color SC emits nearly exclusively green light after pyridine treatment, and its PL and absorption spectra are both shifted to shorter wavelengths (Figure 5), consistent with partial oxidation of the NCs.

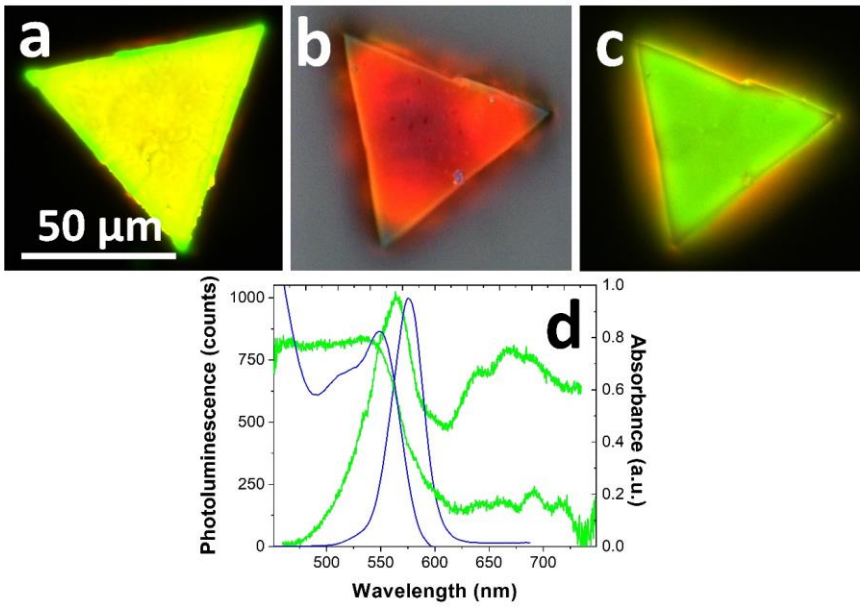

Figure 5. *(a) Fluorescence image of a supercrystal formed from 4.4-nm CdSe nanocrystals before pyridine treatment. (b,c) Reflected light optical micrograph (b) and corresponding fluorescence image (c) of a supercrystal after pyridine treatment. (d) Absorption and photoluminescence spectra measured from a single supercrystal before (longer wavelength) and after (shorter wavelength) pyridine treatment.*

These results indicate that the green and orange regions of the SC are composed, respectively, of NCs that have and have not been partially oxidized. This, in turn, suggests that there are two

sub-populations of NCs that are differently subject to oxidation. Since it is known that the synthesis method that we followed can lead to NCs with both ZB and W phases, we hypothesize that the oxidized and un-oxidized NCs correspond to NCs terminated differently as a result of co-existence of two different phases such W and ZB (or pseudo-ZB,{Washington, 2012 #722}, a phase with a high desity of stacking faults). Previous reports have indicated that ZB and W cadmium chalcogenide NCs have different ligand coverages.[51] For example, NMR studies on CdS NCs of similar sizes revealed that CdS NCs with ZB structure had lower ligand coverage by a factor of 4 as compared to NCs with W structure.[51] The "green" NCs thus most likely have a surface characteristic to ZB crystal structure, which results in a ligand distribution that protects them less against oxidation than the majority of NCs with W crystal structure. Since the complete crystallization takes weeks, oxidation of these ZB or pseudo-ZB NCs can readily occur during the crystallization process.

Alternatively, it is possible that the "green" NCs have some of their surface atoms displaced upon mixing of the NC solution with non-solvent. Leaching of the atoms from NCs as a result of solvent/non-solvent purification was previously reported,[52] and the stoichiometry of cadmium chalcogenides are known to be dynamic in nature and depend on various parameters, including solvents and non-solvents used to purify NCs.[53] On the other hand, CdSe NCs synthesized using reaction conditions similar to those in this work and dissolved in chloroform did not show any change in size and stoichiometry upon extensive ligand removal using methanol.[54] Therefore, oxidation of less protected CdSe NCs is likely to be the main reason responsible for the green emission from these NCs.

The different ligand distribution on the ZB NCs can also lead to them having slightly higher colloidal stability than W NCs, so that they precipitate out of solution later and are deposited at

Formatted: Font color: Red, Highlight

Formatted: Font color: Red, Highlight

Formatted: Font color: Red

Formatted: Font color: Red, Highlight

Formatted: Highlight

Formatted: Highlight

the edges of the SCs. The lower ligand coverage around ZB NCs{Davis, 2017 #734} can provide higher solvation of the ligand shells and thus lower entropy gain through NC interactions (as compared to W NCs with higher ligand coverage) when the colloidal solution is destabilized.[37] Previously, it was shown that high ligand densities are associated with ligand and solvent ordering resulting a deep attractive minima near contact.{Widmer-Cooper, 2016 #829} In turn, at low surface coverage the ligand are random

It worth noting that a significant blue shift of 12 nm and considerable broadening, by 15 nm, compared to the initial NC colloidal solution was recently reported for CdSe SCs assembled by evaporation of CdSe NC solution.[55] Importantly, in that study, CdSe NCs were prepared following the recipe that leads to the synthesis of monodispese CdSe NCs with one or more ZB stacking faults along the c axis. [27] Although the authors did not explain the observed blue shift, their results are in agreement with the progressive oxidation of individual CdSe NCs.

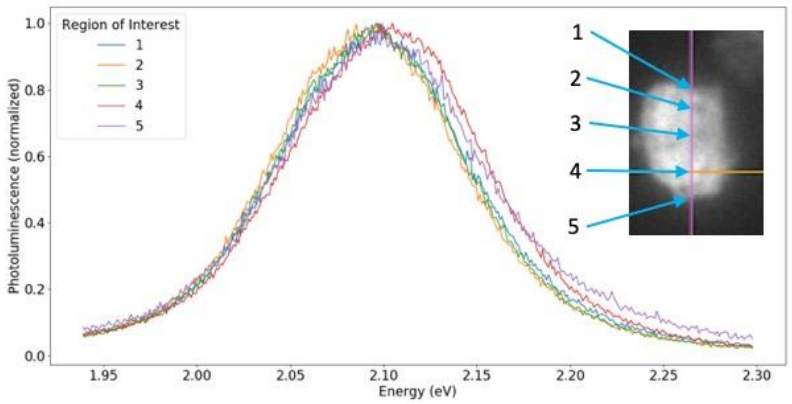

Figure 6. *Spatially-resolved photoluminescence spectra from a single supercrystal formed from 4.9-nm CdSe nanocrystals that were synthesized at 380 °C. Spectra were measured from five*

different points on the nanocrystal, as indicated in the inset, with a spatial resolution of approximately 200 nm.

Our spectroscopic and structural data are all consistent with the hypothesis that the "orange" and "green" regions correspond to NCs with two types of surfaces. Bimodal nature of the observed phenomenon points out to the assumption that it can be associated with co-existence of two different CdSe crystal structures. To further test this hypothesis, we assembled SCs form CdSe NCs synthesized under conditions that provide a better control over the phase.[4] Specifically, we use a higher-temperature synthesis, which has been found to favor the formation of a single W phase of CdSe.[56-57] While there is a discrepancy in literature in the ZB-W transition temperatures{Fedorov, 1991 #828} the general trend is that the higher synthesis temperature favors the formation of thermodynamically stable W phase of CdSe.{Fedorov, 1991 #828}{Nan, 2012 #389}{Washington, 2012 #722} Therefore we assembled ~4.9 nm CdSe NCs synthesized at 380 ^{o}C[4] into SCs, following the same procedure used for assembly of CdSe NCs synthesized at 310 ^{o}C.[19] No noticeable shift of the PL spectra was observed across an individual SC (Figure 6), supporting the hypothesis that the appearance of differently-colored domains is associated with the polymorphism of CdSe NCs.

Formatted: Font color: Red, Highlight
Formatted: Font color: Red, Highlight
Formatted: Font color: Red, Highlight
Formatted: Font color: Red, Highlight
Formatted: Font color: Red, Highlight
Formatted: Font color: Red
Formatted: Highlight
Formatted: Highlight
Formatted: Highlight
Formatted: Highlight

CONCLUSIONS

Assembly of monodisperse CdSe nanocrystals into three-dimensional supercrystals by the controlled oversaturation method leads to SCs with distinct regions whose photoluminescence and absorption are shifted to the red and to the blue, respectively, compared to the NCs in solution. Red-shifted PL has been widely observed in SCs, but the appearance of domains with blue-shifted absorption PL has not been discussed previously. The appearance of blue-shifted domains occurs

only in assemblies of CdSe NCs synthesized at lower temperatures (~310 ^{o}C) and cannot be detected in SCs assembled from CdSe NCs synthetized at higher temperatures (~380 ^{o}C). Since CdSe NCs, especially larger ones, tends to present in both polymorph phases and the energy difference between them is low, it is likely that the green-emitting (blue-shifted) regions result from the small fraction of ZB CdSe or pseudo-ZB NCs present in the ensemble of primarily wurtzite NCs.[58] Our observation

The polytypism of CdSe and other II-VI NCs has important implications for several aspects of NC development and application, particularly the growth of inorganic shells and the synthesis of semiconductor heterostructures.[26, 33, 59] It has been highly challenging to directly identify polytypism or to quantify the fraction of ZB nanocrystals in a majority-W population because of the dynamic nature of the ZB-W transition and similarity of the lattice parameters for the two phases.[25, 58] The segregation of NCs in SCs according to their crystalline form and the corresponding blue-shift of emission from the ZB NCs provide a straightforward method for visualizing and quantifying polytypism.

METHODS

Materials: Toluene, isopropanol (i-PrOH), diphenyl ether, ethanol, *n*-hexane, trioctylphosphine oxide (TOPO), hexadecylamine (HDA), octadecylphosphonic acid (ODPA) bis(trimethylsilyl)sulfide ($(TMS)_2S$), and sulfur were all purchased from Sigma-Aldrich and were at least of ACS purity. Trioctylphosphine (TOP) and 1,2-hexadecandiol were obtained from Fluka. 1,2-dichlorobenzene was purchased from Across Chemicals. 4-inch Si wafers used for growing

the SCs were obtained from Silicon Quest International, Inc. (Santa Clara, CA). The Si wafers were diced into 4 mm wide strips with a wafer dicing saw. Glass test tubes (0.8 cm I.D. by 10 cm long) used for SCs growth were obtained from Fisher Scientific.

Nanocrystals Synthesis: 4.6 and 4.4 nm CdSe NCs stabilized with TOPO/TOP/HDA and TOPO/TOP/ODPA were synthesized according to the protocol described in Ref. 19. 4.9 nm CdSe NCs were synthesized at 380 ^{o}C.[4] Samples for TEM characterization were prepared by placing 1-2 μL of a diluted (0.1 mg/mL) solution in toluene on a carbon-coated copper grid (Ted-Pella). The excess solvent was removed after 10 s with filter paper.

Preparation of Nanocrystal Supercrystals: The SCs were prepared by the method of slow destabilization of NCs with a non-solvent.[19] In a typical preparation, a single strip of Si or ITO-coated glass was placed vertically in a vertically positioned glass test tube, and 0.5 mL of a moderately concentrated NC solution (~$1x10^{12}$ NCs/mL) in toluene was added to the bottom with a micro-pipettor. Subsequently, 0.8 ml of i-PrOH was gently added on top of the NC solution, avoiding intermixing of the two solutions. The tubes were then sealed with Parafilm and allowed to sit undisturbed for a week. After a complete diffusional intermixing of the solvents, the solutions were carefully withdrawn with Pasteur pipettes and discarded. The substrates were removed, air-dried, and stored for subsequent characterization.

NC films were obtained by evaporation of the same toluene solutions on the surface of ITO-coated glass.

Characterization Methods: Transmission-electron microscope (TEM) images were obtained using a FEI Tecnai F30 field-emission analytical TEM operating at an acceleration voltage of 300

kV. High-resolution scanning-electron microscopy (SEM) images were obtained with an FIB FEI Nova 600 NanoLab SEM operated at 18 keV accelerating voltage.

Optical images were obtained with a Zeiss Axio Imager microscope. Fluorescence images were collected with an excitation light source with wavelengths between 320 nm and 460 nm, and with emission collected for wavelengths above 465 nm.

Confocal microscope images and cross-sections were collected using a Zeiss LSM 510 Meta confocal microscope. The particles were excited using 488 nm or 561 nm laser light and emission was monitored in the ranges of 500 – 550 nm or 575 – 625 nm.

Raman spectra were measured on a Renishaw inVia Raman microscope with excitation wavelength of 514 or 613 nm, power of 5 mW, and a spot size of ~ 1 μm. All spectra were measured using a 100X microscope objective to focus the laser excitation onto the samples and to collect the scattered light.

Spatially resolved spectra were measured on a home-built inverted microscope. For spatially resolved photoluminescence (PL) spectra, the sample was illuminated through the microscope objective with a short-wavelength (< 500 nm) laser focused to a diffraction-limited spot (approximately 200 nm spot size), and emitted light was collected through the same objective and sent to a grating spectrometer with CCD-camera detector. Time-resolved PL was measured by using the time-correlated single-photon detection technique in place of the spectrometer. For spatially resolved absorption spectra, the sample was illuminated in transmission mode by a bright-field condenser, and specific spots on the sample were selected for measurement by using the entrance slit of the spectrometer and by selecting pixels on the array detector. The measured transmitted spectra were normalized by spectra measured away from the superlattices to obtain absorption spectra.

The small-angle X-ray scattering (SAXS) data were acquired at the 12-ID-B beamline of the Advanced Photon Source in the Argonne National Laboratory. The X-ray beam had an energy of 14 keV, or wavelength $\lambda = 0.8856$ Å, and size of 10×10 μm. Each spot was exposed to the beam for 1 s. The sample to detector distance was approximately 2 m. Absolute intensity was calculated using water as a standard.

Acknowledgments

We thank Prof. Emily Weiss (Northwestern University) for helpful conversations. Work at the Center for Nanoscale Materials and the Advanced Photon Source was supported by the U.S. Department of Energy, Office of Science, Office of Basic Energy Sciences, under Contract No. DE-AC0206CH-11357.

Supporting Information Available: Figures S1 – S5. This material is available free of charge via the Internet at http://pubs.acs.org.

REFERENCES:

1. Murray, C. B., Norris, D.J., Bawendi, M.G., Synthesis and characterization of nearly monodisperse CdE (E = sulfur, selenium, tellurium) semiconductor nanocrystallites *J. Am. Chem. Soc*. **1993,** *115* (19), 8706-8715.
2. Murray, C. B.; Kagan, C. R.; Bawendi, M. G., Self-Organization of CdSe Nanocrystallites into Three-Dimensional Quantum Dot Superlattices. **1995,** *270* (5240), 1335-1338.
3. Talapin, D. V.; Nelson, J. H.; Shevchenko, E. V.; Aloni, S.; Sadtler, B.; Alivisatos, A. P., Seeded Growth of Highly Luminescent CdSe/CdS Nanoheterostructures with Rod and Tetrapod Morphologies. *Nano Letters* **2007,** *7* (10), 2951-2959.
4. Carbone, L.; Nobile, C.; De Giorgi, M.; Sala, F. D.; Morello, G.; Pompa, P.; Hytch, M.; Snoeck, E.; Fiore, A.; Franchini, I. R.; Nadasan, M.; Silvestre, A. F.; Chiodo, L.; Kudera, S.;

Cingolani, R.; Krahne, R.; Manna, L., Synthesis and Micrometer-Scale Assembly of Colloidal CdSe/CdS Nanorods Prepared by a Seeded Growth Approach. *Nano Letters* **2007,** *7* (10), 2942-2950.
5. Abécassis, B.; Tessier, M. D.; Davidson, P.; Dubertret, B., Self-Assembly of CdSe Nanoplatelets into Giant Micrometer-Scale Needles Emitting Polarized Light. *Nano Letters* **2014,** *14* (2), 710-715.
6. Antanovich, A.; Prudnikau, A.; Matsukovich, A.; Achtstein, A.; Artemyev, M., Self-Assembly of CdSe Nanoplatelets into Stacks of Controlled Size Induced by Ligand Exchange. *The Journal of Physical Chemistry C* **2016,** *120* (10), 5764-5775.
7. Jana, S.; de Frutos, M.; Davidson, P.; Abécassis, B., Ligand-induced twisting of nanoplatelets and their self-assembly into chiral ribbons. *Science Advances* **2017,** *3* (9), e1701483.
8. Kim, D.; Bae, W. K.; Kim, S.-H.; Lee, D. C., Depletion-Mediated Interfacial Assembly of Semiconductor Nanorods. *Nano Letters* **2019,** *19* (2), 963-970.
9. Boles, M. A.; Engel, M.; Talapin, D. V., Self-Assembly of Colloidal Nanocrystals: From Intricate Structures to Functional Materials. *Chemical Reviews* **2016,** *116* (18), 11220-11289.
10. Murray, C. B., Kagan, C.R., Bawendi M.G. , Synthesis and characterization of monodisperse nanocrystals and close-packed nanocrystal assemblies. *Annual Review of Materials* **2000,** *30*, 545-610.
11. Shevchenko, E. V.; Talapin, D. V.; Kotov, N. A.; O'Brien, S.; Murray, C. B., Structural diversity in binary nanoparticle superlattices. *Nature* **2006,** *439*, 55.
12. Dong, A.; Chen, J.; Vora, P. M.; Kikkawa, J. M.; Murray, C. B., Binary nanocrystal superlattice membranes self-assembled at the liquid–air interface. *Nature* **2010,** *466*, 474.
13. Baker, J. L.; Widmer-Cooper, A.; Toney, M. F.; Geissler, P. L.; Alivisatos, A. P., Device-Scale Perpendicular Alignment of Colloidal Nanorods. *Nano Letters* **2010,** *10* (1), 195-201.
14. Rainò, G.; Becker, M. A.; Bodnarchuk, M. I.; Mahrt, R. F.; Kovalenko, M. V.; Stöferle, T., Superfluorescence from lead halide perovskite quantum dot superlattices. *Nature* **2018,** *563* (7733), 671-675.
15. Shevchenko, E. V.; Talapin, D. V.; Rogach, A. L.; Kornowski, A.; Haase, M.; Weller, H., Colloidal Synthesis and Self-Assembly of CoPt3 Nanocrystals. *Journal of the American Chemical Society* **2002,** *124* (38), 11480-11485.
16. Talapin, D. V.; Shevchenko, E. V.; Kornowski, A.; Gaponik, N.; Haase, M.; Rogach, A. L.; Weller, H., A New Approach to Crystallization of CdSe Nanoparticles into Ordered Three-Dimensional Superlattices. *Advanced Materials* **2001,** *13* (24), 1868-1871.
17. Podsiadlo, P.; Krylova, G.; Lee, B.; Critchley, K.; Gosztola, D. J.; Talapin, D. V.; Ashby, P. D.; Shevchenko, E. V., The Role of Order, Nanocrystal Size, and Capping Ligands in the Collective Mechanical Response of Three-Dimensional Nanocrystal Solids. *Journal of the American Chemical Society* **2010,** *132* (26), 8953-8960.
18. Chen, J.; Lim, B. K.; Lee, E. P.; Xia, Y., Shape-controlled synthesis of platinum nanocrystals for catalytic and electrocatalytic applications. *Nano Today* **2009,** *4*, 81-95.
19. Talapin, D. V., Rogach, A.L., Kornowski, A., Haase, M., Weller, H., Highly Luminescent Monodisperse CdSe and CdSe/ZnS Nanocrystals Synthesized in a Hexadecylamine−Trioctylphosphine Oxide−Trioctylphospine Mixture. *Nano Lett.* **2001,** *1* (4), 207-211.
20. Rupich, S. M.; Shevchenko, E. V.; Bodnarchuk, M. I.; Lee, B.; Talapin, D. V., Size-Dependent Multiple Twinning in Nanocrystal Superlattices. *Journal of the American Chemical Society* **2010,** *132* (1), 289-296.

21. Talapin, D. V., Shevchenko, E. V., Murray, C. B., Titov, A. V., Kral, P., Dipole-Dipole Interactions in Nanoparticle Superlattices. *Nano Lett.* **2007,** *7*, 1213-1219
22. Shevchenko, E. V.; Talapin, D. V.; Murray, C. B.; O'Brien, S., Structural characterization of self-assembled multifunctional binary nanoparticle superlattices. . *Journal of the American Chemical Society* **2006,** *128*, 3620-3637.
23. Paik, T.; Diroll, B. T.; Kagan, C. R.; Murray, C. B., Binary and Ternary Superlattices Self-Assembled from Colloidal Nanodisks and Nanorods. *Journal of the American Chemical Society* **2015,** *137* (20), 6662-6669.
24. Manna, L.; Milliron, D. J.; Meisel, A.; Scher, E. C.; Alivisatos, A. P., Controlled growth of tetrapod-branched inorganic nanocrystals. *Nature Materials* **2003,** *2* (6), 382-385.
25. Yeh, C.-Y.; Lu, Z. W.; Froyen, S.; Zunger, A., Zinc-blende--wurtzite polytypism in semiconductors. *Physical Review B* **1992,** *46* (16), 10086-10097.
26. Huang, J.; Kovalenko, M. V.; Talapin, D. V., Alkyl Chains of Surface Ligands Affect Polytypism of CdSe Nanocrystals and Play an Important Role in the Synthesis of Anisotropic Nanoheterostructures. *Journal of the American Chemical Society* **2010,** *132* (45), 15866-15868.
27. Yu, W. W.; Peng, X., Formation of High-Quality CdS and Other II–VI Semiconductor Nanocrystals in Noncoordinating Solvents: Tunable Reactivity of Monomers. *Angewandte Chemie* **2002,** *41* (13), 2368-2371.
28. Mahler, B.; Lequeux, N.; Dubertret, B., Ligand-Controlled Polytypism of Thick-Shell CdSe/CdS Nanocrystals. *Journal of the American Chemical Society* **2010,** *132* (3), 953-959.
29. Chai, Y.; Lu, J.; Li, L.; Li, D.; Li, M.; Liang, J., TEOA-induced in situ formation of wurtzite and zinc-blende CdS heterostructures as a highly active and long-lasting photocatalyst for converting CO2 into solar fuel. *Catalysis Science & Technology* **2018,** *8* (10), 2697-2706.
30. Yang, Y. A.; Wu, H.; Williams, K. R.; Cao, Y. C., Synthesis of CdSe and CdTe Nanocrystals without Precursor Injection. *Angewandte Chemie* **2005,** *44* (41), 6712-6715.
31. Wu, F.; Zhang, Z.; Zhu, Z.; Li, M.; Lu, W.; Chen, M.; Xu, E.; Wang, L.; Jiang, Y., Fine-tuning the crystal structure of CdSe quantum dots by varying the dynamic characteristics of primary alkylamine ligands. *CrystEngComm* **2018,** *20* (31), 4492-4498.
32. Soni, U.; Arora, V.; Sapra, S., Wurtzite or zinc blende? Surface decides the crystal structure of nanocrystals. *CrystEngComm* **2013,** *15* (27), 5458-5463.
33. Wang, X.; Chen, S.; Thota, S.; Wang, Y.; Tan, H.; Tang, M.; Quan, Z.; Zhao, J., Anisotropic Arm Growth in Unconventional Semiconductor CdSe/CdS Nanotetrapod Synthesis Using Core/Shell CdSe/CdS as Seeds. *The Journal of Physical Chemistry C* **2019,** *123* (31), 19238-19245.
34. Kaushik, A. P.; Clancy, P., Solvent-driven symmetry of self-assembled nanocrystal superlattices—A computational study. *Journal of Computational Chemistry* **2013,** *34* (7), 523-532.
35. Waltmann, C.; Horst, N.; Travesset, A., Capping Ligand Vortices as "Atomic Orbitals" in Nanocrystal Self-Assembly. *ACS Nano* **2017,** *11* (11), 11273-11282.
36. Si, K. J.; Chen, Y.; Shi, Q.; Cheng, W., Nanoparticle Superlattices: The Roles of Soft Ligands. *Advanced Science* **2018,** *5* (1), 1700179.
37. Lee, B.; Littrell, K.; Sha, Y.; Shevchenko, E. V., Revealing the Effects of the Non-solvent on the Ligand Shell of Nanoparticles and Their Crystallization. *Journal of the American Chemical Society* **2019,** *141* (42), 16651-16662.
38. Zeng, X.; Liu, F.; Fowler, A. G.; Ungar, G.; Cseh, L.; Mehl, G. H.; Macdonald, J. E., 3D Ordered Gold Strings by Coating Nanoparticles with Mesogens. *Advanced Materials* **2009,** *21* (17), 1746-1750.

39. Guo, S.; Li, D.; Zhu, H.; Zhang, S.; Markovic, N. M.; Stamenkovic, V. R.; Sun, S., FePt and CoPt Nanowires as Efficient Catalysts for the Oxygen Reduction Reaction. *Angewandte Chemie International Edition* **2013,** *52* (12), 3465-3468.
40. Macfarlane, R. J.; Lee, B.; Jones, M. R.; Harris, N.; Schatz, G. C.; Mirkin, C. A., Nanoparticle Superlattice Engineering with DNA. *Science* **2011,** *334* (6053), 204-208.
41. Cho, J.; Kim, Y. J.; Kim, T.-J.; Park, B., Zero-strain intercalation cathode for rechargeable Li-ion cell. *Angew. Chem. Int., Ed.* **2001,** *40*, 3367-3369.
42. Das, T. K.; Ilaiyaraja, P.; Sudakar, C., Coexistence of strongly and weakly confined energy levels in (Cd,Zn)Se quantum dots: Tailoring the near-band-edge and defect-levels for white light emission. *Journal of Applied Physics* **2017,** *121* (18), 183102.
43. Rabani, E.; Hetényi, B.; Berne, B. J.; Brus, L. E., Electronic properties of CdSe nanocrystals in the absence and presence of a dielectric medium. *The Journal of Chemical Physics* **1999,** *110* (11), 5355-5369.
44. Wuister, S. F.; Donegá, C. d. M.; Meijerink, A., Local-field effects on the spontaneous emission rate of CdTe and CdSe quantum dots in dielectric media. *The Journal of Chemical Physics* **2004,** *121* (9), 4310-4315.
45. Hansen, J.; Pusey, P. N.; Warren, P. B.; Yodh, A. G.; Lin, K.; Crocker, J. C.; Dinsmore, A. D.; Verma, R.; Kaplan, P. D., Entropically driven self-assembly and interaction in suspension. *Phylosophical Transaction of the Royal Society A* **2001,** *359* (1782), 921-937.
46. Zaitseva, N.; Dai, Z. R.; Leon, F. R.; Krol, D., Optical properties of CdSe superlattices. *Journal of the American Chemical Society* **2005,** *127* (29), 10221-10226.
47. Banerjee, S.; Jia, S.; Kim, D. I.; Robinson, R. D.; Kysar, J. W.; Bevk, J.; Herman, I. P., Raman Microprobe Analysis of Elastic Strain and Fracture in Electrophoretically Deposited CdSe Nanocrystal Films. *Nano Letters* **2006,** *6* (2), 175-180.
48. Manner, V. W.; Koposov, A. Y.; Szymanski, P.; Klimov, V. I.; Sykora, M., Role of Solvent–Oxygen Ion Pairs in Photooxidation of CdSe Nanocrystal Quantum Dots. *ACS Nano* **2012,** *6* (3), 2371-2377.
49. Hines, D. A.; Becker, M. A.; Kamat, P. V., Photoinduced Surface Oxidation and Its Effect on the Exciton Dynamics of CdSe Quantum Dots. *The Journal of Physical Chemistry C* **2012,** *116* (24), 13452-13457.
50. Luo, X.; Liu, P.; Truong, N. T. N.; Farva, U.; Park, C., Photoluminescence Blue-Shift of CdSe Nanoparticles Caused by Exchange of Surface Capping Layer. *The Journal of Physical Chemistry C* **2011,** *115* (43), 20817-20823.
51. Davis, J. L.; Chalifoux, A. M.; Brock, S. L., Role of Crystal Structure and Chalcogenide Redox Properties on the Oxidative Assembly of Cadmium Chalcogenide Nanocrystals. *Langmuir* **2017,** *33* (37), 9434-9443.
52. Mizrahi, M. D.; Krylova, G.; Giovanetti, L. J.; Ramallo-López, J. M.; Liu, Y.; Shevchenko, E. V.; Requejo, F. G., Unexpected compositional and structural modification of CoPt3 nanoparticles by extensive surface purification. *Nanoscale* **2018,** *10* (14), 6382-6392.
53. Anderson, N. C.; Hendricks, M. P.; Choi, J. J.; Owen, J. S., Ligand Exchange and the Stoichiometry of Metal Chalcogenide Nanocrystals: Spectroscopic Observation of Facile Metal-Carboxylate Displacement and Binding. *Journal of the American Chemical Society* **2013,** *135* (49), 18536-18548.
54. Morris-Cohen, A. J.; Donakowski, M. D.; Knowles, K. E.; Weiss, E. A., The Effect of a Common Purification Procedure on the Chemical Composition of the Surfaces of CdSe Quantum

Dots Synthesized with Trioctylphosphine Oxide. *The Journal of Physical Chemistry C* **2010,** *114* (2), 897-906.
55. Ushakova, E. V.; Cherevkov, S. A.; Volgina, D.-O. A.; Zakharov, V. V.; Komissarenko, F. E.; Shcherbakov, A. A.; Hogan, B. T.; Baldycheva, A.; Fedorov, A. V.; Nabiev, I. R.; Baranov, A. V., From colloidal CdSe quantum dots to microscale optically anisotropic supercrystals through bottom-up self-assembly. *Journal of Materials Chemistry C* **2018,** *6* (47), 12904-12911.
56. Ansar, S. M.; Kitchens, C. L., Impact of Gold Nanoparticle Stabilizing Ligands on the Colloidal Catalytic Reduction of 4-Nitrophenol. *ACS Catalysis* **2016,** *6* (8), 5553-5560.
57. Christodoulou, S.; Vaccaro, G.; Pinchetti, V.; De Donato, F.; Grim, J. Q.; Casu, A.; Genovese, A.; Vicidomini, G.; Diaspro, A.; Brovelli, S.; Manna, L.; Moreels, I., Synthesis of highly luminescent wurtzite CdSe/CdS giant-shell nanocrystals using a fast continuous injection route. *Journal of Materials Chemistry C* **2014,** *2* (17), 3439-3447.
58. Ludescher, L.; Dirin, D. N.; Kovalenko, M. V.; Sztucki, M.; Boesecke, P.; Lechner, R. T., Impact of Crystal Structure and Particles Shape on the Photoluminescence Intensity of CdSe/CdS Core/Shell Nanocrystals. *Frontier in Chemistry* **2019,** *6* (672).
59. Gao, Y.; Peng, X., Crystal Structure Control of CdSe Nanocrystals in Growth and Nucleation: Dominating Effects of Surface versus Interior Structure. *Journal of the American Chemical Society* **2014,** *136* (18), 6724-6732.